Modeling of Benchmark 2; The Oslo group

F. Løvholt, G. Pedersen and J. Kim

July 10, 2017

1 The tsunami models

1.1 Model 1 - GloBouss

GloBouss is a depth averaged model based on the standard Boussinesq equations, including higher order dispersion terms, Coriolis terms, and numerical hydrostatic correction terms [9, 5, 6]. The numerical formulation is based on a staggered Arakawa C-grid computational stencil, solved iteratively employing an ADI method. GloBouss is formulated in both Cartesian and geographical coordinates. GloBouss is mainly a tsunami propagation model designed for simulating dispersive tsunami propagation over large distances in the open ocean, and lacks features such as drying and wetting, and therefore cannot be used to compute inundation. Tsunami sources are handled either through hot start conditions by giving the surface elevation and depth averaged velocity fields as input, or by a series of sources and sinks through the temporal rate of change of the water depth. To accommodate non-hydrostatic effects due to time dependent depth perturbations of short horizontal scales, the tsunami generation is also coupled to a linear, full potential filter based on [3]. For submarine landslide tsunamis, the full potential filter integrates and adds the response water surface response due to the landslide as a function of time. This is done by adding a source term q to the momentum equation

$$\frac{\partial \eta}{\partial t} = -\nabla \cdot \{(h + \eta)\mathbf{v}\} + q, \tag{1}$$

where η, h and $\mathbf{v}$ are the surface elevation, equilibrium depth and depth-averaged horizontal velocity, respectively. In a full set of Boussinesq equations higher order, non-hydrostatic terms will arise from temporal depth changes also in the momentum equations. Such terms are presented, for instance, in [8] where they are also included in a benchmark test. However, for short landslides, such as in the present benchmark 2, these terms will not improve the performance, but they may ruin the hybrid method of section 2.2 where all non-hydrostatic effects during generation are included through the computation of q.

1.2 Model 2 - BoussClaw

BoussClaw is a new Boussinesq type model of similar mold as Funwave-TVD and Coulwave-TVD, but with a different Boussinesq formulation [4]. In particular, the dispersion term is simpler and not fully nonlinear, as robustness is given priority over high formal order. It is an extension of GeoClaw [1], and solves the Boussinesq- type equations by [10], modified into conservative form. The BoussClaw model employ a finite volume technique for the NLSW part

of the equations and a finite difference discretization in fractional steps for the additional terms such as dispersion terms, of both standard and higher order. BoussClaw is an operational tsunami model that incorporates drying wetting formulations which allow for computation of dry land inundation, as well as Manning type friction terms. During inundation and near shore propagation, the dispersive terms are omitted, and the model is switched to NLSW. Tsunami sources are handled either through hot start conditions by giving the surface elevation and depth averaged velocity fields as input, or by modifying the bathymetry in the momentum equation for each time step. To accommodate non-hydrostatic effects during tsunami generation from a time dependent source such as a landslide, modifications to the bathymetry is necessary. In this model the total flow depth $H = h + \eta$ is the primary unknown, together with $\mathbf{v}$. Then the forcing from the time dependent bottom appear in last term, which is spelled out, of the the momentum equation

$$\frac{\partial(H\mathbf{v})}{\partial t} = -\nabla \left\{ H\mathbf{v}^2 + g\frac{1}{2}H^2 \right\} + gH\nabla h + ... \tag{2}$$

2   The landslide tsunami source representation

2.1   The direct implementation

A standard way of implementing a landslide tsunami source in a long wave model is

$$q = -\frac{\partial h}{\partial t}.$$

For a fast bottom variation, as an earthquake, this will give a similar result as copying the bottom uplift on the surface. For a landslide as short as the one in benchmark 2, this procedure will give very inaccurate results, as shown below.

2.2   The hybrid potential flow/long wave source implementation

Features of a bottom source that is not long in comparison to the local depth will not be conveyed directly to the surface as assumed in the preceding section. In principle full potential theory then must be employed to obtain the surface response. On the other hand, the result is that shorter features of the source are smeared out to yield waves that are long enough to be within the realm of dispersive long wave equations [2, 7]. Hence, we employ a hybrid model that that employs full potential theory for the surface response, while long wave equations are used for the wave dynamics. To this end we employ the Green function for the transfer of an impulsive bottom source distribution to the surface elevation from [3] to obtain q from $-\frac{\partial h}{\partial t}$ according to

$$q(x, y, t) = -\int\limits_{-\infty}^{\infty} \int\limits_{-\infty}^{\infty} h(x', y', t))^{-2} \frac{\partial h(x', y', t)}{\partial t} G\left(\frac{\sqrt{(x-x')^2 + (y-y')^2}}{h(x', y', t)}\right) dx'\, dy', \tag{3}$$

where G is the normalized Green function

$$G(r) = \frac{1}{2\pi} \int\limits_{0}^{\infty} \frac{m\mathrm{J}_0(mr)}{\cosh m} dm = \frac{1}{\pi} \sum_{n=0}^{\infty} \frac{(-1)^n(2n+1)}{\{(2n+1)^2 + r^2\}^{\frac{3}{2}}}. \tag{4}$$

The function G decays exponentially as $r \to \infty$ and the integrals in (3) converge rapidly. To compute (4) the bottom uplift rate is discretized one a fine Cartesian grid, with increments

$\Delta x_g, \Delta y_g$ and for each cell a source strength D_{ij} is defined. This should optimally equal $-\partial h/\partial t$ integrated over the cell. Herein we use only the mid-point formula, even though better accuracy could be obtained by modifying this at the edges of the slide body. The computed q is discretized on a grid $(x_n, y_n) = (n\Delta x, m\Delta y) = \vec{r}_{nm}$ which is, normally, much coarser. The discrete counterpart to (3), at location n, m, becomes

$$q_{nm} = -\sum_i \sum_j \frac{1}{h_{ij}^2} \sigma_{ij} D_{ij} G(|\vec{r}_{nm} - \vec{r}_{ij}|/h_{ij}), \tag{5}$$

where i, j refers to the cells of the uplift grid and σ_{ij} is a correction factor, explained below. Due to the decay of G only the contributions from limited ranges in i and j, for which $|\vec{r}_{ij} - \vec{r}_{nm}| < Bh_{ij}$ need to be taken into account. In the simulations herein we have used $B = 5.0$. The factor σ_{ij} is defined according to

$$1 = \frac{\sigma_{ij}\Delta x\Delta y}{h_{ij}^2} \sum_n \sum_m G(|\vec{r}_{nm} - \vec{r}_{ij}|/h_{ij}),$$

where the sums are over all pairs n, m for which q_{nm} are given contribution from $D_{i,j}$ in the truncated series in (5). This ensures volume conservation. When the grid increments are much smaller than Bh_{ij} the factor σ_{ij} is close to unity. For a landslide moving in a channel, side wall effects may be accounted for by introducing mirror sources. However, such effects are only noticeable for the deeper slide positions in benchmark 2. In principle (5) is valid only for constant depth. However, if the horizontal depth variation small, equation (5) is a good approximation in non-uniform depth as well. The application of (5) with the GloBouss model are shown agree very well with full potential theory (both generation and propagation) in [7].

The transformed source may also be applied in the BoussClaw model, but in an incomplete manner. The q as obtained above is then used to define an analogue depth, $\hat{h}$, through $\partial \hat{h}/\partial t = -q$. This depth is then used in the momentum equation 2 of BoussClaw. The source distribution over the surface will then be well presented, but the modified bathymetry will not be correct.

3   Simulations of Benchmark 2

In benchmark 2 the bottom may be expressed as $h = h_b(x) - \hat{\zeta}(x - x_s(t), y)$, and $\hat{\zeta}(\xi, y)$ represents the horizontal projection of the slide body, ζ, which is $0.395\,\mathrm{m} \times 0.680\,\mathrm{m}$. The h_b of starting positions are between $0.14\,\mathrm{m}$ and $27\,\mathrm{m}$, while the maximum depth is $1.8\,\mathrm{m}$. Hence, at the beginning the landslide box is longer than the depth, albeit not by an order of magnitude, while it becomes much smaller than the depth as it moves down the plane. As a consequence, $q = -\partial h/\partial t = \frac{\mathrm{d}x_s}{\mathrm{d}t}\partial\hat{\zeta}/\partial\xi$, i.e. copying the seabed change directly to the water surface, produces waves that are very different from those from q as obtained by equation (5), in particular in deeper regions. This is illustrated in figure 1. Furthermore, we observe that q from (5) may be computed with much relaxed resolution and that it, unlike $\partial\hat{\zeta}/\partial\xi$, is continuous, both of which are beneficial from a numerical point of view.

Time series for the initial slide depths $d = 61\,\mathrm{mm}$ and $d = 120\,\mathrm{mm}$ are shown in figures 2 and 3, respectively. There is good to excellent agreement between experiments and both models offshore, even though there are markedly larger differences for BoussClaw. For gauge 1, on the other hand, the models substantially underestimate the leading depression, in particular for the $d = 61\,\mathrm{mm}$. Non-linear effects are just barely visible for the leading wave (all gauges) while they slightly affect the second wave.
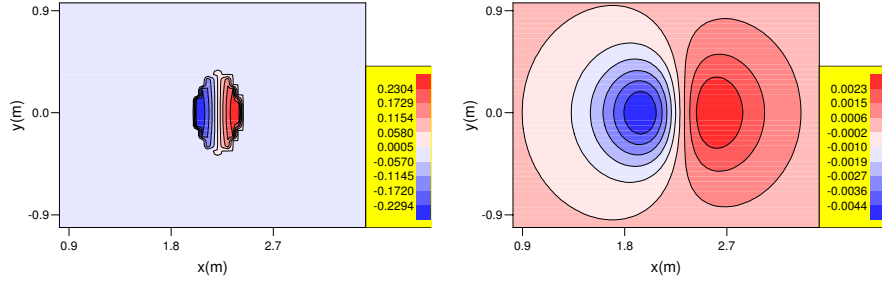
Figure 1: Source distribution for the benchmark 2 landslide starting at $x = 0.605\,\mathrm{m}$ (depth $80\,\mathrm{mm}$) at $t = 1.875\,\mathrm{s}$, when the slide speed is $1.39\,\mathrm{m/s}$. The equilibrium depth at the slide center is then $0.59\,\mathrm{m}$. Left panel: $-\partial h/\partial t$, right panel: q as obtained by (5). The ragged appearance in the left panel reflects the inadequacy of a good resolution ($\Delta x = 0.045\,\mathrm{m}$) for q, when applied to $-\partial h/\partial t$.
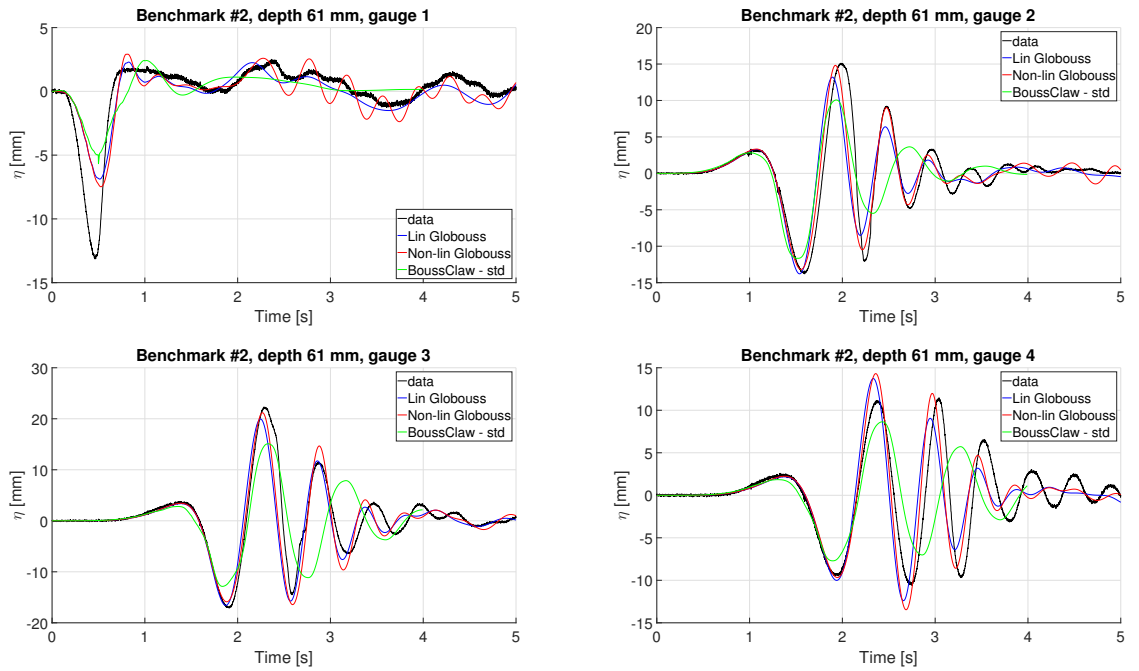
Figure 2: Time series for $d = 61\,\mathrm{mm}$
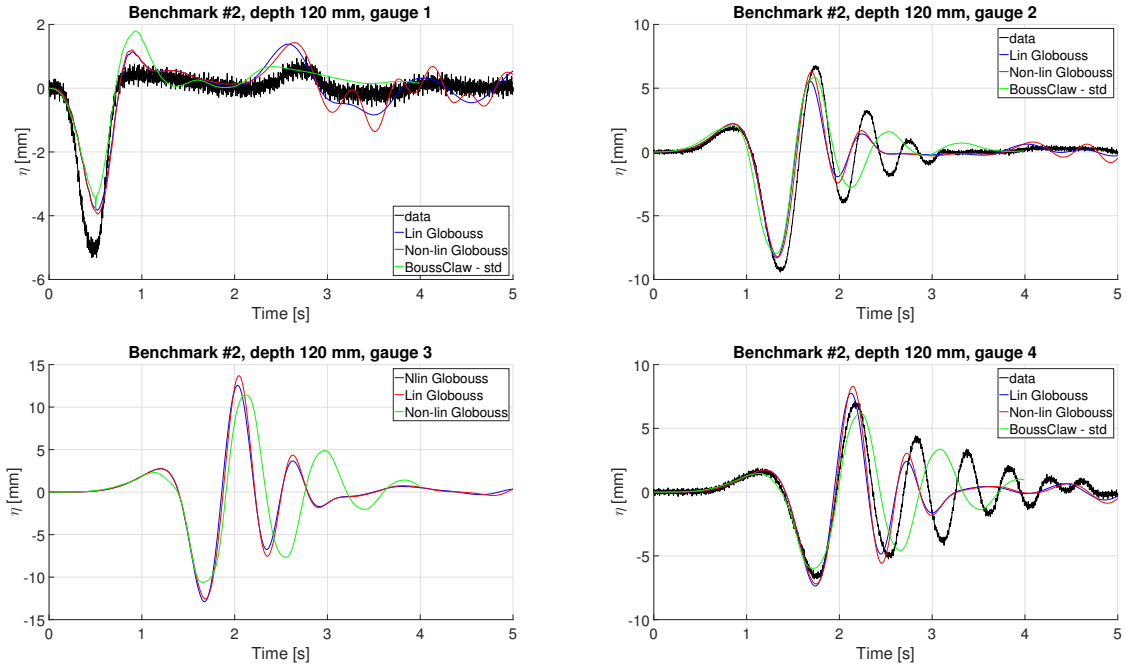
Figure 3: Time series for $d = 120\,\text{mm}$

4   Remarks

The hybrid model generally works well, except at small times for the shallow gauge 1 where it yields a too low initial depression. When results for all gauges are taken into account (not shown) there is also a weak tendency that events with higher value of t_0 (e.g. $d = 140\,\text{mm}$ and $d = 189\,\text{mm}$) yield a better general fit with experiments, possibly due to longer induced wavelength. There is also a slightly improved fit for larger d, even for gauge 1.

Equation (3) is intrinsically linear in the sense that the sink/source distribution is applied at the undisturbed sea bed. This is a rather crude approximation at the start of the slide motion, in particular for $d = 61\,\text{mm}$, for which the slide is thicker than half the undisturbed water depth. Presumably, this is part of the explanation for the under representation of the leading depression at gauge 1. Plane tests (not shown), including a full potential theory model for both generation and propagation, supports this. However, the effects are different in 2D and 3D and further investigation is needed to reach a firm conclusion. The modification of the geometry may be taken into account in all other terms in GloBouss, but the effect on the solution is moderate. In the presented simulations we have simply set $\hat{\zeta} = \zeta$. A corrected $\hat{\zeta}$, for which the slope has been taken into consideration, has been tested, but gave only minor differences. The formula (3) itself is valid for constant depth. Plane tests, where slides of similar length and height and speed have been simulated with both GloBouss and full potential theory (not shown) points to an error of up to 10%, say.

Equation (3) does not take the sidewalls or the beach into account. These effects are generally small, but may be noticeable in deeper water close to the tank sidewalls. The effects of the sidewalls may for some simple geometries, such as in benchmark 2, be included by mirror sources. However, the generalization to more complex geometries is not straightforward. The original

benchmark 2 parameters are still used. As pointed out before the workshop the slide description given in the benchmark specification and the underlying articles include inconsistencies, which also has bearing on the comparisons, in addition to other factors such as the gap between the slide body and the beach etc.

References

[1] Clawpack Development Team. Clawpack software, 2016. Version 5.3.1.

[2] S. Glimsdal, G. K. Pedersen, C. B. Harbitz, and F. Løvholt. Dispersion of tsunamis; does it really matter? *Natural hazards and earth system sciences*, 13(6):1507–1526, 2013.

[3] K. Kajiura. The leading wave of a tsunami. *Bulletin of the Earthquake Research Institute*, 41:535–571, 1963.

[4] J. Kim, G. Pedersen F. Løvholt, and R. Leveque A Boussinesq type extension of the GeoClaw model - a study of wave breaking phenomena applying dispersive long wave models. *Coastal Eng.*, 122:75–86, 2017.

[5] F. Løvholt, G. Pedersen, and G. Gisler. Oceanic propagation of a potential tsunami from the La Palma Island. *J. Geophys. Res.*, 113:C09026, 2008. DOI:10.1029.

[6] F. Løvholt, G. Pedersen, and S. Glimsdal. Coupling of dispersive tsunami propagation and shallow water coastal response. *The Open Oceanography Journal*, 4:71–82, 2010. DOI:10.2174/1874252101004010071.

[7] F. Løvholt, G. Pedersen, C.B. Harbitz, S. Glimsdal, and J. Kim. On the characteristics of landslide tsunamis. *Phil. Trans. R. Soc. A*, 373:20140376, 2015.

[8] G. Pedersen. A Lagrangian model applied to runup problems. In P. L.-F. Liu, H. Yeh, and C. E. Synolakis, editors, *Advanced Numerical Models for Simulating Tsunami Waves and Runup*, volume 10 of *Advances in Coastal and Ocean Engineering*, pages 311–314. World Scientific Publishing, Singapore, 2008.

[9] G. Pedersen and F. Løvholt. Documentation of a global Boussinesq solver. Preprint Series in Applied Mathematics 1, Dept. of Mathematics, University of Oslo, Norway, 2008. **URL:** http://www.math.uio.no/eprint/appl_math/2008/01-08.html.

[10] Hemming A Schäffer and Per A Madsen. Further enhancements of Boussinesq-type equations. *Coastal Engineering*, 26(1):1–14, 1995.